

IHTC14-8888

First and Second Law Analysis of Fluid Flow in the Regenerator of Pulse Tube Refrigerators

F. Roshanghalb

M.Sc. Student,

School of Mechanical Engineering, Sharif
University of Technology, Tehran, Iran
f.roshanghalb@gmail.com

M. H. Saidi

Professor,

School of Mechanical Engineering, Sharif
University of Technology, Tehran, Iran
saman@sharif.edu

A. Jafarian

PhD,

School of Mechanical Engineering, Sharif
University of Technology, Tehran, Iran
a_jafarian@mehr.sharif.edu

F. Imanimehr

Payam-e-Nour University, Tehran, Iran
f.imanimehr@yahoo.com

M. Asadi

M.Sc.,

School of Mechanical Engineering, Sharif
University of Technology, Tehran, Iran
m_asadi@mech.sharif.ir

ABSTRACT

The objective of the present work is to analyze the performance of the regenerator of pulse tube refrigerators. Hydrodynamic and thermal behavior of the regenerator is investigated in this respect. To consider the system performance, a system of conservation equations including two energy equations for the regenerator as a porous media is employed. The present model considers one dimensional periodic unsteady compressible flow in the regenerator. The conservation equations are transformed by implementing the volumetric average scheme. Method of harmonic approximation is employed to derive an analytical solution. To explore the system performance, net energy flow and entropy generation minimization technique is applied in order to calculate the regenerator first and second law efficiencies. The effect of geometry and operating key parameters on the regenerator performance are considered as well.

Keywords: Oscillatory flow, Porous media, Entropy generation, Regenerator

INTRODUCTION

Pulse tube refrigerators have been extensively studied in recent years. These systems have some advantages over other regenerative cryogenic cycles such as having no moving parts

at its cold head, mechanical simplicity, high reliability, low cost and so on. Figure 1 shows a schematic view of a double inlet pulse tube refrigerator. The concept of basic pulse tube refrigerator was primarily introduced by Gifford et al.[1]. Mikulin [2] examined the orifice pulse tube refrigerator seeking higher efficiency. Furthermore, Zhu [3] achieved a new constructional solution to increase the orifice pulse tube refrigerator efficiency through adding an extra bypass, namely double inlet pulse tube refrigerator. The improvement of double inlet pulse tube refrigerator was achieved by implementing a bypass between the central zones of the Pulse tube and that of the thermal regenerator. This improvement led to a new configuration named Multi Bypass Pulse Tube Refrigerator [4]. Further efforts have been performed during the recent years to improve the performance of the pulse tube refrigerators. The regenerator of pulse tube refrigeration system as a necessary component plays an important role in the refrigeration performance. Regarding the analysis of the regenerator, several efforts have already been performed. These efforts are categorized into the subjects of type of materials, experiments and modeling. Waele et al.[5] considered the energy and mass conservation equations in the case of steady state pulse tube with a linear expression for flow resistance of the material. Before Waele, Xiao et al. proposed a model, neglecting the

conduction effect. In addition, Swift et al. and Roach et al., presented their analysis based on thermo acoustic effect and phasor analysis, respectively [5]. Further more Kashani, et al. [6] proposed an optimization program for modeling of the pulse tube coolers. Gary et al. derived REGEN3.2 model and Gedeon presented SagePulse Tube Model [7]. Lewis et al. considered the effect of regenerator geometry on pulse tube refrigerator performance [8]. Harvey et al. proposed a comparative evaluation of numerical models for cryocooler regenerators [9]. In spite of numerous mentioned efforts to analyze and optimize the performance of pulse tube refrigerators, a few works have been performed to consider the dissipative phenomena in the regenerator. Regenerator is the main source of entropy generation and lost work [10, 11]. In addition, due to the complexity of oscillatory flow equations, proposed numerical and CFD models, usually take considerable time to perform system optimization. In the present paper, the energy flow and entropy generation phenomena are investigated considering a complete system of compressible oscillating flow equations. An analytical technique is employed in our study which has the ability to perform rapid optimization. Regenerator first and second law efficiencies are considered simultaneously for system optimization.

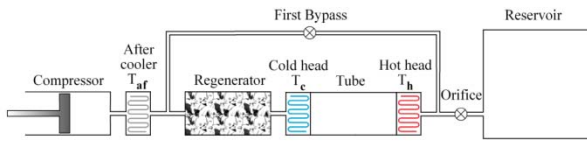


Fig. 1. A schematic view of double inlet pulse tube refrigerator

NOMENCLATURE

A (m^2)	area
C ($J/kg.K$)	specific heat capacity
C_f	inertia coefficient
D (m)	diameter
e (J)	internal energy
En (J/kg)	gas enthalpy
h ($W/m^2.K$)	heat transfer coefficient
H (W)	energy flow
k ($W/m.K$)	thermal conductivity
K (m^2)	permeability
L (m)	length
\dot{m} (kg/s)	mass flow rate
Nk	conductivity enhancement
Nu	Nusselt number
P (bar)	pressure
R ($J/kg.K$)	gas constant
Re	Reynolds number
Real	real part
\dot{S} ($W/K.m^3$)	entropy generation rate
S (m)	displacement length
t (s)	time
T (K)	temperature
u (m/s)	velocity
V (m^3)	volume

\dot{W} (W)	rate of work transfer
x (m)	longitudinal position

Subscripts & Superscripts:

0	reference state
1	first order
v	constant volume
s	solid
H	hot end
C	cold end
p	constant Pressure
w	wall
g	gas
s	solid
sg	solid to gas
r	regenerator
CHX	cold heat exchanger
HHX	hot heat exchanger
m	mean value
c	cross section
t	tube
gen	generation
sys	system
pass	passage
h	hydraulic
*	non dimensional

Greeks:

ρ (kg/m^3)	density
ω (1/s)	angular velocity
μ ($kg/m.s$)	dynamic viscosity
ν (m^2/s)	kinematic viscosity
τ	solid tortosity
ϵ	porosity
ϕ	phase shift angle

MATHEMATICAL FORMULATION

Mass, momentum, energy conservation and the equation of state represent the compressible gas flow in the regenerator. Here, the gas flow in the regenerator is considered as one dimensional periodic compressible.

$$\frac{\partial \rho_g}{\partial t} + \nabla \cdot (\rho_g \vec{u}_g) = 0 \quad (1)$$

$$\frac{\partial (\rho_g \vec{u}_g)}{\partial t} + \nabla \cdot (\rho_g \vec{u}_g \vec{u}_g) = -\nabla P_g + \frac{1}{3} \nabla (\mu_g \nabla \vec{u}_g) + \nabla \cdot (\mu_g \nabla \vec{u}_g) \quad (2)$$

$$\frac{\partial (\rho_g e_g)}{\partial t} + \nabla \cdot (\rho_g \vec{u}_g e_g - k_g \nabla T_g) = 0 \quad (3)$$

$$(\rho C)_s \frac{\partial T_s}{\partial t} - \nabla \cdot (k_s \nabla T_s) = 0 \quad (4)$$

$$P_g = f(\rho_g, e_g) \quad (5)$$

$$T_g = f(\rho_g, e_g) \quad (6)$$

The main assumptions used in the present model are as follows:

1. The outer sidewall of the regenerator is thermally insulated.
2. Ideal gas assumption is made and flow regime is laminar.
3. The regenerator length is much larger than the regenerator radius, thus, the entrance effects are neglected.

Under the above assumptions as well as implementing the volumetric average scheme, the conservation equations and equation of state in the case of one-dimensional flow in the x-direction leads to [7]:

$$\frac{\partial \rho_g}{\partial t} + \frac{\partial(\rho_g u_g)}{\partial x} = 0 \quad (7)$$

$$\frac{\partial(\rho_g u_g)}{\partial t} + \frac{\partial}{\partial x}(\rho_g u_g^2) + \frac{\partial P}{\partial x} + \frac{\mu \varepsilon}{K} u_g + \rho_g u_g^2 \frac{\varepsilon^2 C_f}{\sqrt{K}} \frac{|u_g|}{u_g} = 0 \quad (8)$$

$$\frac{\partial(\rho_g u_g)}{\partial t} + \frac{\partial}{\partial x} \left(\rho_g u_g E n_g - N_k k_g \frac{\partial T_g}{\partial x} \right) - h_{sg} A_s (T_s - T_g) = 0 \quad (9)$$

$$(\rho C)_s \frac{\partial T_s}{\partial t} - \frac{\partial}{\partial x} \left[k_s \tau_s \frac{\partial T_s}{\partial x} \right] + \frac{\varepsilon}{1 - \varepsilon} h_{sg} A_s (T_s - T_g) = 0 \quad (10)$$

$$P_g = \rho_g R T_g \quad (11)$$

Boundary conditions on the velocity and temperature are given as follows:

$$x = 0 \Rightarrow \begin{cases} u = \omega S_H \text{Real}(e^{i\omega t}) \\ k_s(1 - \varepsilon) \frac{\partial T_s}{\partial x} = h_H(T_s - T_{HHX}) \\ T_g = T_{HHX} \end{cases} \quad (12)$$

$$x = L \Rightarrow \begin{cases} u = \omega S_C \text{Real}(e^{i\omega(t-\varphi)}) \\ k_s(1 - \varepsilon) \frac{\partial T_s}{\partial x} = h_C(T_{CHX} - T_s) \\ T_g = T_{CHX} \end{cases} \quad (13)$$

Three convection heat transfer coefficients are introduced, while investigating the thermal behavior of the regenerator. These three coefficients characterize the heat transfer between the regenerator and surrounding, the gas and internal surface of the regenerator wall and the heat transfer between gas and matrix, respectively. Several formulations can be found in the literature [12-19] for the heat transfer coefficient between the gas and matrix. Nika et al. [16], Reza et al. [17] and Prenel [18] employed the following correlation in the case of packed wire screens used in the Stirling engine.

$$Nu = \frac{h D_h}{k_g} = p Re_h^q, \quad p = 0.33, \quad q = 0.67 \quad (14)$$

In this research we have used equation (14) to calculate the heat transfer coefficient between the gas and matrix. where, in the above equation:

$$Re_h = \frac{\dot{m} D_h}{\mu_g A_{pass}} \quad (15)$$

The permeability K is expressed in terms of the pressure drop coefficient C_f and the Reynolds number Re_h [12, 17].

$$K = \frac{2\varepsilon D_h^2}{Re_h C_f} \quad \text{where, } C_f = \frac{a}{Re_h^c} + b, \quad \text{and } Re_h = \frac{\dot{m} D_h}{\mu_g A_{pass}} \quad (16)$$

The value of the coefficients a, b and c for different situations can be found in [17].

SOLUTION PROCEDURE

Method of harmonic approximation is applied to derive an analytical solution. In this technique, variables are expressed as a sum of mean values plus higher order terms, the terms of order higher than first-order are neglected in this study. A product of two first order terms is assumed to be a second-order, while a product of a mean value and a first order term still remains first order.

$$X(x, t) = X_m + \text{Real}[X_1(x)e^{i\omega t}] \quad (17)$$

where, the real parts of the complex variables are designated by the symbol Real. Substituting the above expressions into the conservation equations and the equation of state, the first order system of equations is obtained. The variables being non-dimensionalized as:

$$x^* = \frac{x}{L}, \quad t^* = \omega t, \quad u^* = \frac{u}{u_0}, \quad T^* = \frac{T}{T_H}, \quad \rho^* = \frac{\rho}{\rho_0}, \quad P^* = \frac{P}{P_0}$$

Expressing the system of first order equations versus non-dimensionalized parameters leads to:

$$\rho_{1g}^* - i\beta_1 \frac{\partial(\rho_{mg}^* u_{1g}^*)}{\partial x^*} = 0 \quad (18)$$

$$\rho_{mg}^* u_{1g}^* - i\beta_2 \frac{\partial P_{1g}^*}{\partial x^*} - i\beta_3 u_{1g}^* = 0 \quad (19)$$

$$i\beta_4 T_{1g}^* \rho_m^* e^{it^*} + \beta_5 \rho_{mg}^* u_{1g}^* \frac{\partial T_{mg}^*}{\partial x^*} e^{it^*} + \frac{\partial}{\partial x^*} (P_{mg}^* u_{1g}^*) e^{it^*} - \beta_6 \left(\frac{\partial^2 T_{mg}^*}{\partial x^{*2}} + \frac{\partial^2 T_{1g}^*}{\partial x^{*2}} e^{it^*} \right) - \beta_7 [(T_{ms}^* - T_{mg}^*) + (T_{1s}^* - T_{1g}^*) e^{it^*}] = 0 \quad (20)$$

$$iT_{1s}^* e^{it^*} - \beta_8 \left(\frac{\partial^2 T_{mg}^*}{\partial x^{*2}} + \frac{\partial^2 T_{1s}^*}{\partial x^{*2}} e^{it^*} \right) + \beta_9 [(T_{ms}^* - T_{mg}^*) + (T_{1s}^* - T_{1g}^*) e^{it^*}] = 0 \quad (21)$$

$$\rho_{1g}^* = \beta_{10} \frac{P_{1g}^*}{T_{mg}^*} - \rho_{mg}^* \frac{T_{1g}^*}{T_{mg}^*} \quad (22)$$

where, dimensionless parameters have been defined in Table 1.

Boundary conditions on velocity and temperature are given as non-dimensionalized form:

$$x^* = 0 \Rightarrow \quad (23)$$

$$\left\{ \begin{array}{l} u^* = \frac{1}{\beta_1} S_H^* \operatorname{Re}(e^{it^*}) \rightarrow \frac{\partial P_{1g}^*}{\partial x^*} = -(\rho_{mg}^* - i\beta_3) i\beta_{11} S_H^* \\ \frac{\partial T_s^*}{\partial x^*} = \beta_{12} (T_s^* - T_{HHX}^*) \\ T_g^* = T_{HHX}^* \end{array} \right.$$

$$x^* = L \Rightarrow \left\{ \begin{array}{l} u^* = \frac{1}{\beta_1} S_C^* \operatorname{Re}(e^{i(t^* - \varphi)}) \rightarrow \frac{\partial P_{1g}^*}{\partial x^*} = -(\rho_{mg}^* - i\beta_3) i\beta_{11} S_C^* e^{-i\varphi} \\ \frac{\partial T_s^*}{\partial x^*} = \beta_{12} (T_s^* - T_{HHX}^*) \\ T_g^* = T_{HHX}^* \end{array} \right. \quad (24)$$

Thermophysical properties of helium gas including specific heat capacity, thermal conductivity and viscosity are obtained from the helium database presented in [20]. In our study the physical properties of the helium gas are considered as a function of mean temperature along the regenerator. These physical data have been formulated by curve fitting. The specific heat capacity and thermal conductivity of the regenerator material have been formulated by curve fitting as well.

According to the results of [5] and [21] and the analysis performed in the present study, the magnitude of the second term in the right hand side of equation (22) is negligibly smaller than the first term. This means that the first order density is significantly a function of the first order pressure rather than temperature. Thus the second term has been neglected in this study.

Since the outer surface of regenerator wall is assumed to be adiabatic, the net energy flow in the longitudinal direction is independent of the position. This fact can be applied to obtain the mean temperature profile of the gas in the regenerator. To simplify the solution procedure we acquired a linear trend for the mean temperature. Net energy flow analysis showed that this profile satisfies the mentioned rule precisely. Therefore we have a system of differential equations in complex form that should be solved to obtain the pressure gradient, density, velocity field and first order temperature distribution of the gas and solid matrix. Following are the steps which have been followed to achieve the solution.

1. Substitute equations (19) and (22) in equation (18) and solve the differential equation numerically to obtain the pressure field and pressure gradient along the regenerator.
2. Put the pressure gradient into equation (19) to obtain the first order velocity.
3. Solve the system of differential equations numerically for first order temperature of the gas and solid matrix after substitution of the first order velocity in equations (24) and (21).
4. Put the first order values obtained from solving the equations (18)-(22) into the equations (16)-(17) to finalize the solution.

The physical parameters and typical values used in the present study are given in Table 2 of appendix A.

ENERGY FLOW ANALYSIS

The amount of loss in a regenerator can be evaluated by the net energy flow through the regenerator. Since the outer surface of the regenerator wall is taken adiabatic, the net energy flow which includes both enthalpy flow by the gas and heat conduction through the regenerator solid phase and the gas can be stated as follows:

$$\dot{H} = \frac{1}{2\pi} \int_0^{2\pi} \left[(\dot{m} C_p T_g) k_s \tau_s A_{pass} \frac{\partial T_s}{\partial x} - k_t A_t \frac{\partial T_t}{\partial x} \right] dt \quad (25)$$

Substitution of harmonic values in the equation and omitting second order terms after non-dimensionalizing the net energy flow equation leads to:

$$\dot{H}^* = \frac{1}{2\pi} \int_0^{2\pi} \left[\rho_{mg}^* T_{mg}^* u_{1g}^* e^{it^*} - \beta_{14} \left(\frac{\partial T_{ms}^*}{\partial x^*} + \frac{\partial T_{1s}^*}{\partial x^*} e^{it^*} \right) \right] dt^* \quad (26)$$

ENTROPY GENERATION AND LOST WORK

The Efficiency is of fundamental importance for the design of pulse tube refrigerators. One of the common criteria used to optimize the performance of the mechanical systems is maximization of the efficiency of 1st law of thermodynamic which here means minimization of the net energy flow. However, this parameter does not consider irreversibility due to viscous, inertial effects and heat flow. The efficiency of 2nd law of thermodynamic can be defined by considering the rate of mechanical energy required to overcome the friction force. On the other hand, the energy loss originated by the viscous dissipation and heat flow must also be included. The 1st and 2nd laws of thermodynamic efficiencies of the regenerator are defined as given by equations (27) and (28).

$$\eta_{1st} = 1 - \frac{\langle \dot{H} \rangle}{\langle \dot{W} \rangle} \quad (27)$$

$$\eta_{2nd} = 1 - \frac{\langle T_0 \dot{S}_{gen} \rangle}{\langle \dot{W} \rangle} \quad (28)$$

where, \dot{W} is the net work transfer rate to the system to overcome the friction forces and symbol $\langle \rangle$ denotes integration over space and one period of time.

In the viscous fluid flow, the entropy generation must consider irreversibility caused by fluid friction, inertia and heat flow. Its explicit form can be obtained from the fluid and entropy balance equations along with the linear constitutive relations for the fluxes of momentum and heat. Non-dimensional equations for the local entropy generation and lost work are as follows:

$$\dot{S}_{g,gen}^* = \frac{1}{T_s^{*2}} \left(\frac{\partial T_g^*}{\partial x^*} \right)^2 - \beta_{15} \frac{u_g^*}{T_g^*} \left(\frac{\partial P_g^*}{\partial x^*} \right) + \beta_{16} \frac{1}{T_s^* T_g^*} (T_s^* - T_g^*)^2 \quad (29)$$

$$\dot{S}_{s,gen}^* = \frac{1}{T_s^{*2}} \left(\frac{\partial T_g^*}{\partial x^*} \right)^2 + \beta_{17} \frac{1}{T_s^* T_g^*} (T_s^* - T_g^*)^2 \quad (30)$$

$$\dot{S}_{sys,gen}^* = \varepsilon \dot{S}_{g,gen}^* (1 - \varepsilon) \dot{S}_{g,gen}^* \quad (31)$$

$$\dot{W}_{lost}^* = \int_0^1 \dot{S}_{sys,gen}^* dx^* \quad (32)$$

where dimensionless parameters in the equations are defined as given in Tables 1 and 3.

Since the second law efficiency considers the whole dissipation produced by irreversibility in the system, it can be employed to optimize the operation of the regenerator section of the pulse tube refrigerators by looking for values of the effective parameters that minimize the entropy generation and so maximize the second law efficiency, η_{2nd} , for the proper operation conditions.

RESULTS

In this section, friction coefficient, interfacial heat transfer, first and second law efficiencies as well as cooling capacity and coefficient of performance of the whole cryocooler cycle of the regenerator, have been investigated.

Figures 2 and 3 display the effect of the regenerator aspect ratio on operating parameters of the cryocooler. It is obvious that cooling capacity, heat transfer coefficient and COP are significant functions of aspect ratio, while first and second law efficiencies and friction coefficient do not change seriously by varying the aspect ratio. The above mentioned figures have been plotted at 35 and 4 Hz frequencies to highlight the frequency influence as well.

Figures 2 and 3 show the same behavior; meanwhile comparison of figures 2 and 3 represents that increasing the frequency from 4 Hz to 35 Hz leads to the increase of the mass flow rate; so that the Reynolds number will increase accordingly. Consequently, according to equation (16) the friction coefficient falls down and the cooling capacity grows up.

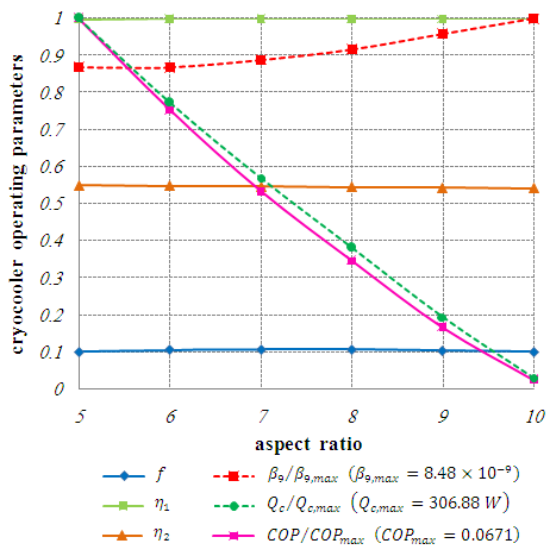


Fig. 2. Cryocooler operating parameters in the regenerator at different aspect ratios (at 35 Hz frequency)

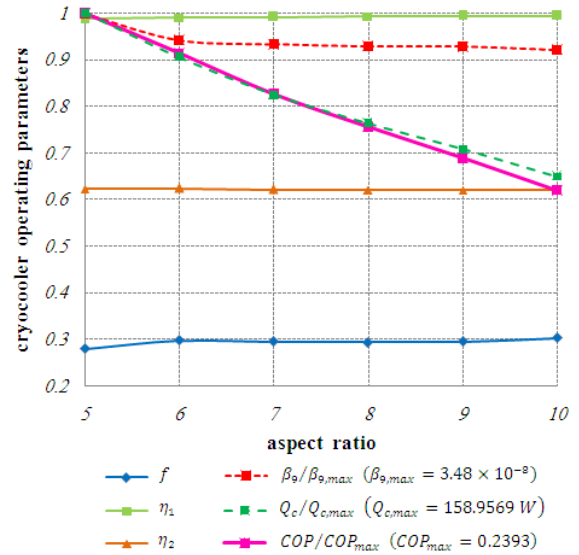


Fig. 3. Cryocooler operating parameters in the regenerator at different aspect ratios (at 35 Hz frequency)

Figures 4 and 5 show the effect of mesh size on operating parameters of cryocooler. In figure 4 all cryocooler operating parameters are normalized relative to their max value except the first law efficiency. Figure 4 shows that increasing the mesh size leads to the increase of friction coefficient and decrease of coefficient of performance. Also it can be concluded that non dimensional heat transfer coefficient takes its maximum value nearly at mesh number of 250. By comparing figure 4 and 5 it is concluded that a sharp increase occurs in compressor power consumption while the frequency increases from 4 Hz to 35 Hz, meanwhile the cooling capacity increases as well. Due to the trade off between the two mentioned parameters COP falls down by increasing the frequency.

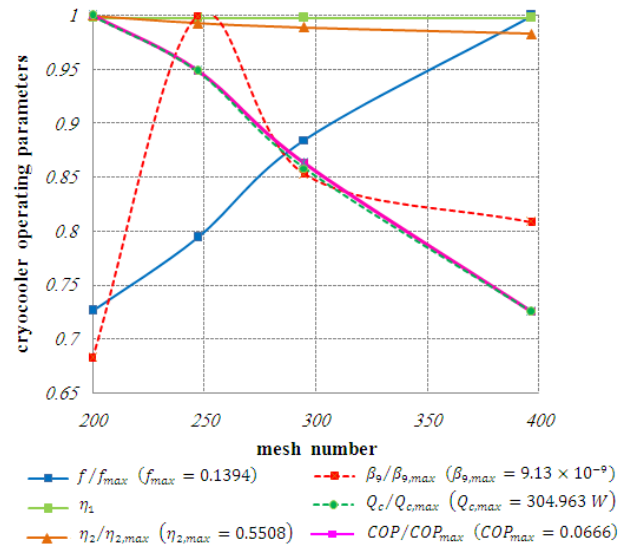


Fig. 4. Cryocooler operating parameters in the regenerator at different aspect ratios (at 35 Hz frequency)

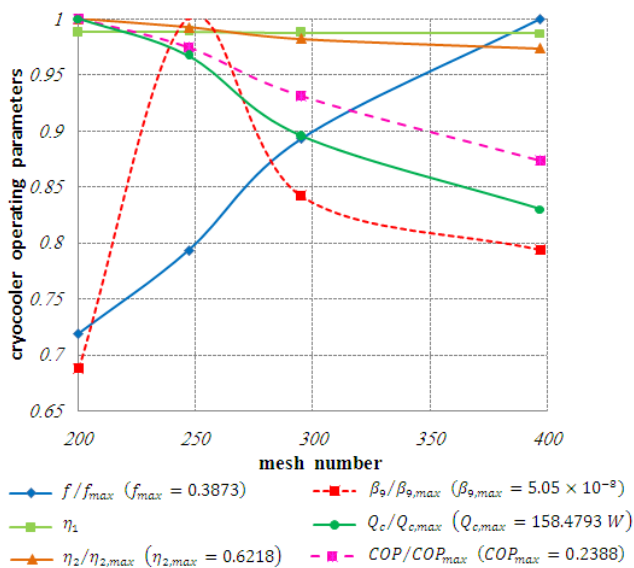


Fig. 5. Cryocooler operating parameters in the regenerator at different aspect ratios (at 35 Hz frequency)

CONCLUSION

A one dimensional model for performance analysis of the regenerator of pulse tube refrigerator has been proposed in this research. Dual energy equation model was adopted in this study to analyze the porous regenerator. The velocity, pressure and temperature fields for the oscillatory flow have been calculated. Furthermore, net energy flow as a loss mechanism in the regenerator has been explored and the method of entropy generation minimization was employed as a powerful technique for system optimization. The influence of geometry and some effective parameters on the first and second law efficiencies of the regenerator was considered as well. Results show that variation of some operating parameters, a different behavior is observed between first and second law efficiencies. Second law efficiency illustrates the total dissipative phenomena in the regenerator which are missed while considering the first law efficiency. Thus the second law efficiency can be employed as a reliable parameter for performance analysis of the regenerator. The system of equations in the proposed model are generally valid and can be applied for different types of pulse tube refrigerators and especially for comparison of regenerator performance between various models such as orifice, double inlet, multi bypass and multi stage systems.

REFERENCES

[1] Popescu, G., Radcenco, V., Gragalian, E. and Ramany Bala, P. "A Critical Review of Pulse Tube Cryogenerator Research", *Int. J. Refrig.* Vol. 24, pp 230-237 (2001).
 [2] Mikulin, EI., Tarasov, AA. and Shkrebyonok, MP. "Low Temperature Expansion Tubes", *Adv. Cryog. Eng.*, pp 629-637 (1984).
 [3] Zhu, SW., Wu, PY. and Chen ZQ. "A Single Stage Double Inlet Refrigerator Capable of Reaching 42 K", *ICEC 13 Proc. Cryogenics*, pp 257-261 (1990).

[4] Cai, JH., Wang, JJ., Zhu, WX. and Zhou, Y. "Experimental Analysis of Double Inlet Principle in Pulse Tube Refrigerator", *Cryogenics* pp 522-525 (1993).
 [5] De Waele, A.T.A.M., Hoojikaas, H.W.G., Steijaert, P.P. and Benschop A.A.J. "Regenerator Dynamics in the Harmonic Approximation", *Cryogenics*, Vol. 38, pp 995-1006 (1998).
 [6] Kashani, A. and Roach, P.R. "An Optimization Program for Modeling Pulse Tube Coolers", *Advances in Cryogenic Engineering*, Vol. 43, Plenum Press, New York (1999).
 [7] Harvey, J. "Oscillatory Compressible Flow and Heat Transfer in Porous Media- Application to Cryocooler Refrigerators", PhD Thesis, Georgia Institute of Technology (2003).
 [8] Lewis, M., Kuriyama, T., Xiao, J., and Radebaugh, R. "Effect of Regenerator Geometry on Pulse Tube Refrigerator Performance", *Advances in Cryogenic Engineering*, Vol. 43. Plenum Press, New York (1999).
 [9] Harvey, J., Desai, P., and Kirkconnell, C., "A Comparative Evaluation of Numerical Models for Cryocooler Regenerators" *Cryocoolers*, Vol. 12, Kluwer Academic, New York, pp 547-554 (2003).
 [10] Neveu, P. and Babo, C. "A Simplified Model for Pulse Tube Refrigeration", *Cryogenics*, Vol. 40, pp 191-201 (2000).
 [11] He, Y.L., Huang, J., Zhao, Ch. F. and Liu, Y.W. "First and Second Law Analysis of Pulse Tube Refrigerator", *Applied Thermal Engineering* Vol. 26, pp 2301-2307 (2006).
 [12] Nika, Ph., and Bailly, Y. "Comparison of Two Models of a Double inlet Miniature Pulse Tube Refrigerator: Part B, Electrical Analogy", *Cryogenics* (42), pp 605-615 (2002).
 [13] Tanaka, M., Yamashita, I., and Chisaka, F. "Flow and Heat Transfer Characteristics of the Stirling Engine Regenerator in an Oscillating Flow", *JMSE Int J Series II*,33(2), pp 283-9 (1990).
 [14] Ju, Y.L. and Wang L., "On the Numerical Design of a New Type of 4 K GM/PT Hybrid Refrigerators", *Cryogenics* (42), pp 533-542 (2002).
 [15] Ju, Y.L., Wang, C. and Zhou, Y. "Numerical Simulation and Experimental Verification of the Oscillating Flow in Pulse Tube Cryocooler", *Cryogenics* (38), pp169 (1998).
 [16] Qiu, L.M., He, Y.L., Gan, Z.H., Zhang, X.B. and Chen G.B. "Regenerator Performance Improvement of a Single-Stage Pulse Tube Cooler Reached 11.1 K", *Cryogenics* (47), pp 49-55 (2007).
 [17] Nika, Ph., Bailly, Y., Jeanot, J.C. and Labachelerie, M. D. "An Integrated Pulse Tube Refrigeration with Micro Exchangers: Design and experiment", *International Journal of Thermal Science*, Vol. 42, pp 1029-1045 (2003).
 [18] Reza, S. and Charles, J. C., "State of the Art in Micro and Meso Scale Heat Exchangers", in: *AES*, Vol. 39, Proc. of the ASME, pp 53-61.
 [19] Prenel, J.P. "Optical Systems for Fluids Mechanics Investigations, Invited paper, in: Proceedings of the Second International Conference on Optical Design and Fabrication", Tokyo, November, pp 129-132 (2000).

- [20] Robert, D. Mc. "Thermodynamic Properties of Helium 4 from 2 to 1500 K at Pressure to 10^8 Pa", J. Phys. Chem. Ref. Data, Vol. 2, No. 4 (1973).
- [21] Beak, S.H., Jeong, E.S. and Jeong, S. "Two-dimensional Model for Tapered Pulse Tubes. Part 1: Theoretical Modeling and Net Enthalpy Flow", Cryogenics (40), pp 379-385 (2000).

APPENDIX A

Table 1- Dimensionless parameters in non dimensional governing equations

Symbol	Definition
β_1	$\frac{u_0}{L\omega}$
β_2	$\frac{P_0}{\rho_0 u_0 L \omega}$
β_3	$\frac{\mu \varepsilon}{K \rho_0 \omega}$
β_4	$\frac{\omega T_H \rho_0 C_v L}{P_0 u_0}$
β_5	$\frac{\rho_0 T_H C_v}{P_0}$
β_6	$\frac{N_k k_g T_H}{P_0 u_0 L}$
β_7	$\frac{h_{sg} A_s T_H L}{P_0 u_0}$
β_8	$\frac{k_s \tau_s}{L^2 \omega (\rho C)_s}$
β_9	$\frac{\varepsilon h_{sg} A_s}{(1-\varepsilon)\omega(\rho C)_s}$
β_{10}	$\frac{P_0}{\rho_0 R_g T_H}$
β_{11}	$\frac{\rho_0 L^2 \omega}{P_0}$
β_{12}	$\frac{h_H L}{k_s (1-\varepsilon)}$
β_{13}	$\frac{h_C L}{k_s (1-\varepsilon)}$
β_{14}	$\frac{(k_s \tau_s A_{pass} + k_t A_t)}{\rho_0 u_0 C_p L}$

β_{15}	$\frac{P_0 u_0 L}{T_H N_k k_g}$
β_{16}	$\frac{L^2 h_{sg} A_s}{N_k k_g}$
β_{17}	$\frac{L^2 h_{sg} A_s \varepsilon}{\tau_s k_s (1-\varepsilon)}$

Table 2- Physical and operating data for a typical pulse tube refrigerator

Symbol	Definition	Value
\bar{k}_g	Gas thermal conductivity	0.1125 Wm ⁻¹ K ⁻¹
\bar{k}_s	Solid thermal conductivity	12 Wm ⁻¹ K ⁻¹
\bar{C}_p	Constant pressure specific heat capacity	5225 Jkg ⁻¹ K ⁻¹
\bar{C}_v	Constant volume specific heat capacity	3125 Jkg ⁻¹ K ⁻¹
\bar{C}_s	Solid heat capacity	368 Jkg ⁻¹ K ⁻¹
$\bar{\mu}$	Dynamic viscosity	147.6×10 ⁻⁷ kg.m ⁻¹ s ⁻¹
$\bar{\rho}_g$	Helium average density	5.95 kg.m ⁻³
ρ_s	Solid density	7800 kg.m ⁻³
u_0	Reference velocity	3.8 m.s ⁻¹
ρ_0	Reference density	3.2 kg.m ⁻³
P_0	Reference pressure	20 bar
\bar{T}_H	Hot end temperature	300 K
\bar{T}_C	Cold end temperature	100 K
P_m	Mean pressure	20 bar
f	Frequency	20 Hz
R_g	Gas constant	2100 J.kg ⁻¹ K ⁻¹
ε	Porosity	0.6536

K	Permeability	$5.20 \times 10^{-11} \text{ m}^2$
d_w	Wire diameter	$5.6 \times 10^{-2} \text{ m}$
D_h	Hydraulic diameter	$9.194 \times 10^{-2} \text{ m}$
S_{pass}	Open Area	$9.74 \times 10^{-5} \text{ m}^2$
A_s	Area Density	$24740.16 \text{ m}^2 \cdot \text{m}^{-3}$
L	Length	0.2 m
t	Regenerator thickness	0.001 m

Table 3- Dimensionless parameters in Eqs. (26), (29), (30) and (32)

Symbol	Definition
\dot{H}^*	$\frac{\dot{H}}{\rho_0 \mu_0 C_p T_H A_{pass}}$
$\dot{S}_{g,gen}^*$	$\frac{\dot{S}_{g,gen}}{N_k k_g / L^2}$
$\dot{S}_{s,gen}^*$	$\frac{\dot{S}_{s,gen}}{k_s \tau_s / L^2}$
\dot{W}_{lost}^*	$\frac{\dot{W}_{lost} L^2}{T_H V_r N_k k_g}$